

Charles University, Faculty of Science
Department of Physical and Macromolecular Chemistry

Univerzita Karlova, Přírodovědecká fakulta
Katedra fyzikální a makromolekulární chemie

Doctoral study programme: Macromolecular chemistry
Doktorský studijní program: Makromolekulární chemie

Summary of the Doctoral thesis
Autoreferát disertační práce



Functionalized hybrid polymer structures for biomedical applications
Funkcionalizované hybridní polymerní struktury pro biomedicínské aplikace

Mgr. Rabyk Mariia

Supervisor/Školitel: RNDr. Petr Štěpánek, DrSc.
Consultant/Konzultant: Mgr. Martin Hrubý, DSc.

Institute of Macromolecular Chemistry AS CR
Ústav makromolekulární chemie AV ČR, v.v.i

Prague 2018

Abstract

This doctoral thesis is dedicated to the synthesis and characterization of novel functionalized hybrid structures for biomedical purposes. The systems reported in this work can be subdivided into the two main groups: natural-based materials and synthetic amphiphilic block copolymers. Both groups were studied as perspective theranostic agents for medical applications. In the first group, natural polysaccharides glycogen and mannan were selected as starting materials for preparation of novel nanoconjugates that exhibit ability for multimodal imaging *in vivo*. Because grafting of natural macromolecules with synthetic polymers generally slows down the biodegradation rate, both polysaccharides were modified in two different ways to form nanoprobe with or without poly(2-methyl-2-oxazoline)s chains. The prepared nanoconjugates were functionalized with *N*-hydroxysuccinimide-activated fluorescence and magnetic resonance imaging labels. The resulting materials were tested both *in vitro* and *in vivo* and were shown to be completely biocompatible, biodegradable and to exhibit some extra benefits in terms of their practical usage in biomedicine. Glycogen was functionalized with allyl and propargyl groups with following freeze-drying from aqueous solutions to form nano- and microfibrillar materials. The presence of both double and triple bonds ensures the possibility of electron radiation crosslinking and modification of resulting polymer with biologically active molecules, respectively. The obtained self-assembled structures reveal a great perspective for wound healing application.

The second part of this thesis is devoted to the preparation and characterization of novel amphiphilic diblock copolymers as a model for studying the micellar behaviour of the complex self-assembled architectures with stimuli-responsive properties. Nitroxide-mediated radical polymerization was used for the synthesis of well-defined diblock copolymers of styrene (S) and 2-dimethylaminoethyl acrylate (DMAEA), where the first block consisted of gradient copolymer of the two monomers and the second one was a homopolymer of DMAEA. As a result, due to the pH- and temperature-responsiveness of DMAEA units, polycationic amphiphilic block copolymers capable of reversible self-assembling behaviour were obtained. Moreover, one chosen copolymer was modified using thiol-ene click reaction and further functionalized with fluorescence label in order to perform the *in vitro* examination and to study its potential for biomedical applications.

All the prepared polymers were characterized using a wide range of methods, including ^1H magnetic resonance and Fourier-transform infrared spectroscopies, size exclusion chromatography and dynamic light scattering. Additionally, for the amphiphilic diblock copolymers small angle neutron scattering was performed to study their solution behaviour.

Keywords: nanomedicine, polysaccharides, glycogen, mannan, nitroxide-mediated radical polymerization, amphiphilic block copolymers, self-assembling.

Abstrakt

Tato dizertační práce se věnuje syntéze a charakterizaci nových hybridních struktur využitelných v biomedicině. Tyto systémy jsou zde rozděleny do dvou hlavních skupin: modifikované přírodní polymery a syntetické amfifilní blokové kopolymery, přičemž obě tyto skupiny byly studovány jako potenciální theranostická činidla pro medicínské aplikace. Co se týče první skupiny, přírodní polysacharidy glykogen a manan byly vybrány jako výchozí materiály pro přípravu nových nanokonjugátů, určených pro multimodální zobrazení *in vivo*. Protože roubování polysacharidů pomocí syntetických polymerů obecně zpomaluje biodegradací procesy, oba polysacharidy byly modifikovány dvěma různými způsoby tak, aby vytvořily „nanosondy“, přičemž jeden způsob využíval roubování pomocí poly(2-methyl-2-oxazolinu). Připravené nanokonjugáty byly funkcionalizovány pomocí *N*-hydroxysukcimidového esteru, díky čemuž výsledné materiály nesly fluorescenční značku a značku pro magnetickou rezonanci. Finální materiály byly testovány *in vitro* a *in vivo*, přičemž bylo zjištěno, že jsou plně biokompatibilní a biodegradovatelné a zároveň vykazují užitečné vlastnosti pro praktické využití v biomedicině. Glykogen byl modifikován tak, aby nesl allylové a propargylové skupiny, a poté byl lyofilizován z vodného roztoku, aby mohl vytvořit nano- a mikrovláknitý materiál. Přítomnost dvojných vazeb v jeho struktuře zajistila možnost zesíťování pomocí β -záření a k tomu přítomnost trojných vazeb umožnila modifikaci tohoto polymeru pomocí biologicky aktivních molekul. Získané samouspořádané struktury byly shledány jako velmi perspektivní materiály pro hojení ran.

Druhá část této práce se zabývá přípravou a charakterizací nových amfifilních diblokových kopolymerů, které slouží jako modely pro studium samouspořádaných komplexů citlivých na vnější podněty. Pro syntézu definovaného diblokového kopolymeru styrenu (S) a 2-dimethylaminoethyl akrylátu (DMAEA) byla použita řízená radikálová polymerizace, přičemž první syntetizovaný blok byl gradientový kopolymer obou monomerů a druhý syntetizovaný blok byl homopolymer DMAEA. Výsledný diblokový polykationtový kopolymer vykazoval reverzibilní chování při změně pH a teploty, což je způsobeno tím, že samotný DMAEA je citlivý na vnější podněty. Nakonec byl vybrán kopolymer s nejužitečnějšími vlastnostmi a jeho potenciál pro biomedicínské aplikace byl studován *in vitro*.

Všechny připravené polymery byly charakterizovány pomocí široké škály metod – ^1H nukleární magnetické rezonance, infračervené spektroskopie, gelové permeační chromatografie či dynamického rozptylu světla. Navíc roztoky amfifilních diblokových kopolymerů byly studovány pomocí malouhlového neutronového rozptylu.

Klíčová slova: nanomedicína, polysacharidy, glykogen, manan, řízená radikálová polymerizace, amfifilní blokové kopolymery, samouspořádání.

List of abbreviations

CNR	contrast to noise ratio
CROP	cationic ring-opening polymerization
DDS	drug delivery system
DLS	dynamic light scattering
DMAEA	2-dimethylaminoethyl acrylate
DOTA	1,4,7,10-tetraazacyclododecane-1,4,7,10-tetraacetic acid
Dy615	Dyomics 615
Ds	dansyl or [5-(dimethylamino)naphthalene-1-sulfonyl]
EPR effect	enhanced permeability and retention effect
FITC	fluorescein 5-isothiocyanate
FLI	fluorescence imaging
FTIR spectroscopy	Fourier transform infrared spectroscopy
GG	glycogen
GM	gadoterate meglumine
IR	infrared
i.v.	intravenous
MN	mannan
MONAMS	<i>N</i> -(<i>tert</i> -butyl)- <i>N'</i> -(1-diethylphosphono-2,2'-dimethyl-propyl)- <i>O</i> -(1-methoxycarbonyl-ethyl)hydroxylamine
MRI	magnetic resonance imaging
MTT	3-(4,5-dimethylthiazol-2-yl)-2,5-diphenyl-tetrazolium bromide
NHS-ester	<i>N</i> -hydroxysuccinimide ester
NMRP	nitroxide-mediated radical polymerization
PBS	phosphate buffer saline
POX	poly(2-methyl-2-oxazoline)
RES	reticuloendothelial system
RGD-peptide	azidopentanoic-GGGRGDSGGGY(¹²⁵ I)-NH ₂ peptide
RNU	Rowett Nude
S	styrene
SANS	small angle neutron scattering
SG1	<i>N</i> -(<i>tert</i> -butyl)- <i>N'</i> -(1-diethylphosphono-2,2'-demethyl-propyl)nitroxide
SEM	scanning electron microscopy
TE	tissue engineering
UV	ultraviolet
ZP	ζ-potential

Contents

1.	Introduction.....	6
2.	Aims of the thesis.....	7
3.	Results and discussion.....	7
3.1.	Polysaccharide-based conjugates for drug delivery and diagnostic purposes.....	7
3.1.1.	Glycogen-based hybrid complexes for cancer diagnostic and therapeutic purposes.....	7
3.1.2.	Mannan-based conjugates for multimodal imaging.....	11
3.2.	Glycogen-based fibrous material for tissue engineering.....	15
3.3.	Synthesis of amphiphilic block copolymers and their modification.....	17
4.	Conclusions.....	22
5.	References.....	23
6.	Curriculum vitae.....	25
7.	List of publications and contributions at conferences.....	26

1. Introduction

Generally nanomaterials are made of inorganic (semiconductors, metals, their oxides and alloys)¹⁻³ or organic (polymers, phospholipids, *etc.*) compounds. A vast number of current researches in macromolecular science are dedicated to perspective materials for preparation of new nanoscale structures for biomedical applications. These substances could be of synthetic, natural or hybrid (consisting of both natural and synthetic components) origin. Each type of these materials has its benefits and drawbacks, but the most clever and reasonable approach lies in using all advantages of natural polymers and adjusting their properties according to the actual needs by combining them with synthetic polymers. Such hybrid substances exhibit biocompatibility and biodegradability and, at the same time, possess a wide range of possible chemical modifications for better defined structures. Moreover, an additional decoration of these hybrid materials with appropriate active compound, *i.e.*, drug, genetic material, dye, contrast agent *etc.*, opens an endless source of new biodegradable systems for medical purposes. Design and preparation of drug delivery systems, development of new diagnostic nanoprobes and preparation of different scaffolds and healing systems for tissue engineering (TE), are the main branches in the wide field of nanomedicine⁴.

Drug delivery systems or diagnostic probes intended for medical application have to fulfil certain requirements. First of all, nanostructures have to be biodegradable, biocompatible, and non-toxic. Second, the material should be present at the site of desired action in sufficiently high concentration and for the appropriate period of time. In preparation of any functional nanomaterial intended for biomedical uses the selection of appropriate precursor plays a critical role. It determines not only physico-chemical properties of final nanostructure, but also regulates its interaction with biological systems. Among the variety of materials used in drug delivery nanomedicine, a special place is dedicated to natural polymers due to their abundance in nature, good biocompatibility, biodegradability and ability for easy modifications. The majority of new systems created for nanomedicine using natural polymers are based on the proteins and polysaccharides⁵⁻⁸. In the last decade, an enormously high interest was devoted to preparation of drug delivery systems (DDS) and different diagnostic probes on the base of biodegradable polysaccharides^{5,9,10}. Despite the beneficial properties of glycogen (GG) it is still underused for the purposes of biomedicine with only a few published studies on the topic, *e.g.* GG has been used for coating of gold nanoparticles and to form hydrogels by enzymatic modification with amylose¹¹. Therefore, in this thesis glycogen was selected as a platform for preparation and characterization of the novel hybrid nanostructures for application in biomedicine as a dual modal contrast agent for fluorescence imaging (FLI) and magnetic resonance imaging (MRI) (with a perspective use in drug delivery and diagnostic field of biomedicine). In addition, recently our group reported on GG fibrous structure formed by simple freeze-drying of its aqueous solution. A fibrous nature of materials to be used for scaffold preparation is especially advantageous for wound healing dressings due to the extremely high porosity and permeability. The ability of GG to form fibers by freeze-drying its aqueous solution was used in this thesis for preparation of the new perspective materials for regenerative medicine.

Mannan (MN) is another biocompatible, biodegradable, non-toxic polysaccharide, which, due to the presence of large number of hydroxyl groups in its structure, can be easily modified to achieve the desired properties. MN is a promising candidate for the development of new polysaccharide-based nanocarriers for biomedical applications due to specific property to target immune cells¹² that exhibits extra advantages for investigation of pathological processes and development of corresponding therapies. In particular, MN-based materials are expected to possess benefits for diagnosis of the sentinel lymph nodes and inflammations

which are heavily infiltrated with macrophages and dendritic cells. Thus, MN was selected as a precursor for development of new multimodal contrasts for lymph nodes visualization.

Moreover, in the area of drug delivery, nanoparticles prepared by self-assembly of synthetic amphiphilic block copolymers were also proved to be fully competitive. This field benefits from the most advanced synthetic developments. Using existing controlled polymerization methods, a big variety of amphiphilic and stimuli-responsive polymers were prepared in the last decade¹³. Supramolecular nanostructures that are formed by self-assembling of material's building blocks through non-covalent interactions are intensively studied nowadays as an extremely promising candidate for different therapeutic purposes¹⁴⁻¹⁶. Nanoassemblies formed by amphiphilic block copolymers are well known as perspective platforms for cancer diagnosis and therapy because of their relatively small size, high loading capacity and prolonged blood circulation¹⁷. Preparation of the novel nanostructures with a more advanced architecture for possible controlled drug release is, therefore, one of the main topics in nanomedicine¹⁸. In this thesis a model for studying the micellar behaviour of the complex self-assembled architectures with stimuli-responsive properties was prepared and characterized.

Therefore, this work is focused on the development of novel nanomaterials for both diagnostic and therapy, using natural nano-scaled materials and self-assembled nanostructures prepared from polymers of both synthetic and biological origin.

2. Aims of the thesis

The main goal of the work was the development of new functionalized hybrid materials based on both natural and synthetic made polymers as theranostic agents for biomedical applications.

The specific goals of the thesis were the following:

1. Synthesis and characterization of new hybrid copolymers based on biodegradable polysaccharides, which can be potentially used for the diagnostics and therapeutics of cancer. As the precursors for this purpose two polysaccharides were chosen: glycogen and mannan.
2. Preparation of a new biodegradable glycogen-based hybrid functional material to be used in tissue engineering.
3. Preparation of the novel diblock stimuli-responsive nanocontainers based on styrene and 2-(dimethylamino)ethyl acrylate, which can be used in biomedicine for delivery of active payload.

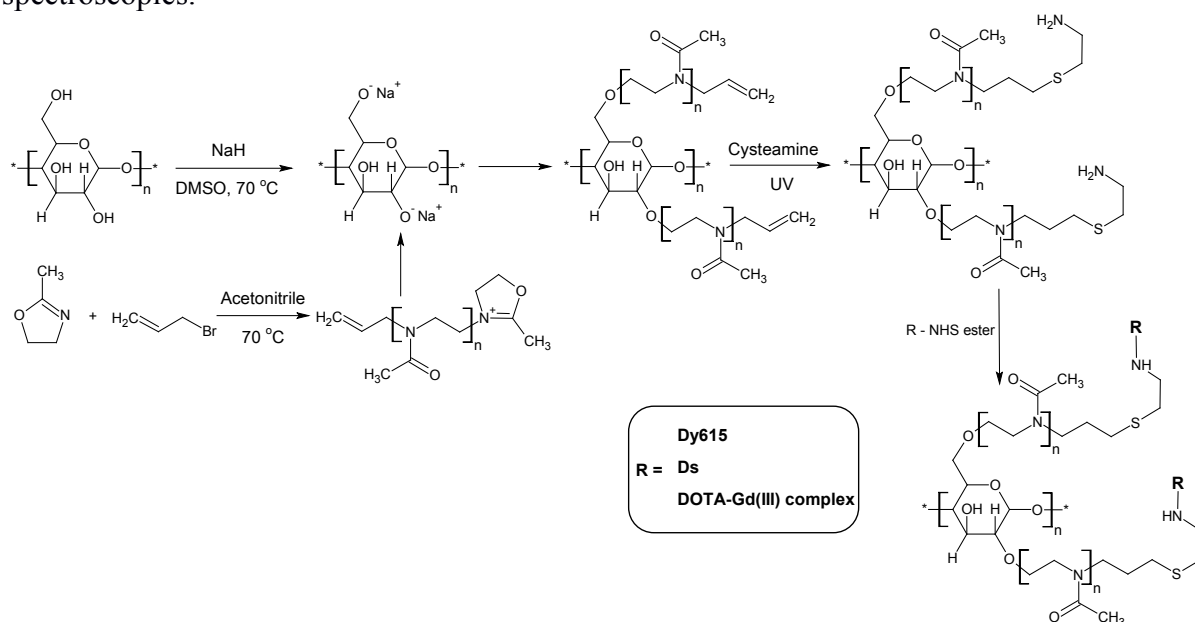
3. Results and discussion

3.1. Polysaccharide-based conjugates for drug delivery and diagnostic purposes

3.1.1. Glycogen-based hybrid complexes for cancer diagnostic and therapeutic purposes

The preparation of dual modal contrast agents from GG were done according to Scheme 1. The glycogen-*graft*-poly(2-methyl-2-oxazoline)s (denoted as GG-POX) were prepared analogously to the previously described procedure¹⁹. The 2-methyl-2-oxazoline was polymerized by cationic polymerization initiated with allyl bromide and then its living ends were terminated by separately prepared glycogen sodium alkoxide. The molecular weight of poly(2-methyl-2-oxazoline) (POX) grafts was determined by mass spectrometry after termination of active chains with water: number-average molecular weight $M_n = 672$ g/mol, polydispersity $D = M_w/M_n = 1.11$, where M_w is the weight-average molecular weight. The formed GG-POX contained vinyl groups that were then further reacted with cysteamine by ultraviolet (UV)-initiated thiol-ene "click" chemistry to introduce primary amino groups to

glycogen conjugates. The latest were subsequently marked with different fluorescent dyes, resulting in fluorescent glycogen conjugates for both *in vitro* and *in vivo* imaging. The structure of conjugates was confirmed by ^1H , ^{13}C NMR and Fourier-transform infrared (FTIR) spectroscopies.



Scheme 1. Synthesis path for glycogen modification with poly(2-methyl-2-oxazoline).

Characterization of the GG-based nanostructures in terms of their hydrodynamic diameter (D_{hyd}) and ζ -potential (ZP) in solution was done by dynamic light scattering (DLS) and electrophoretic mobility measurements, respectively. For these experiments, the neat GG and the all synthesized conjugates were dissolved in aqueous or phosphate buffer saline (PBS) medium at concentration 1 mg/mL. The performed chemical modification of neat GG increased its D_{hyd} from 54 to 79 nm in the case of aqueous solution and from 49 to 77 nm in the case of PBS solution (Table 1). This increase in hydrodynamic size can be explained by the presence of ionic groups, originating from dansyl (Ds), fluorescein 5-isothiocyanate (FITC), DOTA or infrared (IR) complexes in the structure of final conjugates, which leads to the mutual repulsion between the same charged moieties and, as a result, in more expanded conformation of macromolecules. Moreover, the changes in ZP values for each product confirm the successful modification of neat polysaccharide. When PBS was used as a solvent, the presence of counter ion layer led to the significant decrease of ZP of all probes and slight decrease of D_{hyd} values compared to those in the water (Table 1).

Table 1. Hydrodynamic diameter and ζ -potential of the final GG-based conjugates obtained by DLS and electrophoretic mobility measurements, respectively.

Sample	D_{hyd} , nm		ζ -potential, mV	
	PBS	H ₂ O	PBS	H ₂ O
GG	49	54	-2.5	-4.5
GG POX-1 Ds	61	68	-1.4	-7.7
GG POX-3 Ds	70	79	-4.8	-45.2
GG Dy615	66	79	0	25
GG DOTA-Gd Dy615	60	72	-10.5	40.2
GG POX-1 FITC	55	58	-3	-36.6
GG IR DOTA-Gd	60	79	3.4	43.8
GG POX_IR DOTA-Gd	77	79	-3.3	7.8

First biological experiments were focused on the dependence of endocytosis rate on glycogen grafting density and were monitored with fluorescence spectroscopy. Generally, the functionalization degree of polysaccharide with synthetic polymer grafts should affect the endocytosis rate of the resulting hybrid system. Indeed, the obtained results shows slower uptake of GG with POX in the structure compared to the non-grafted one. Moreover, higher content of polyoxazoline chains leads to the further decrease in endocytosis rate, because grafted POX chains make the glycogen core more hidden for cells. These results are in a good agreement with the previous studies reported in literature focused on dextrin succinylation, where dextrin with a higher level of modification shows slower biodegradation rate^{20,21}. Decreased rate of GG uptake with a higher content of POX may also contribute to prolonged blood circulation that brings additional benefits for the preparation of long time circulating contrast agents.

A classic colorimetric assay using 3-(4,5-dimethylthiazol-2-yl)-2,5-diphenyl-tetrazolium bromide (MTT) dye was used to study toxicity of our polymers. The test showed non-toxicity of all used concentrations of GG-POX-1-FITC, while the levels of cells viability were similar to the control cells. The viability for cells incubated with unmodified glycogen was also not affected during the study. Therefore, results from the MTT assays confirmed the non-toxicity of native glycogen as well as of the prepared GG-based conjugates.

After *in vitro* tests, the probe with fluorescent label Dyomics 615 (Dy615), denoted as GG-Gd_Dy615, was administered into experimental animals for investigation of *in vivo* distribution, degradation and elimination of conjugates using optical imaging. Average radiant efficiency in case of experimental mice was by one order higher compared to the negative control (Figure 1A), and in 24 hours after administration of GG-based conjugates fluorescence the signal was still detectable (Figure 1B).

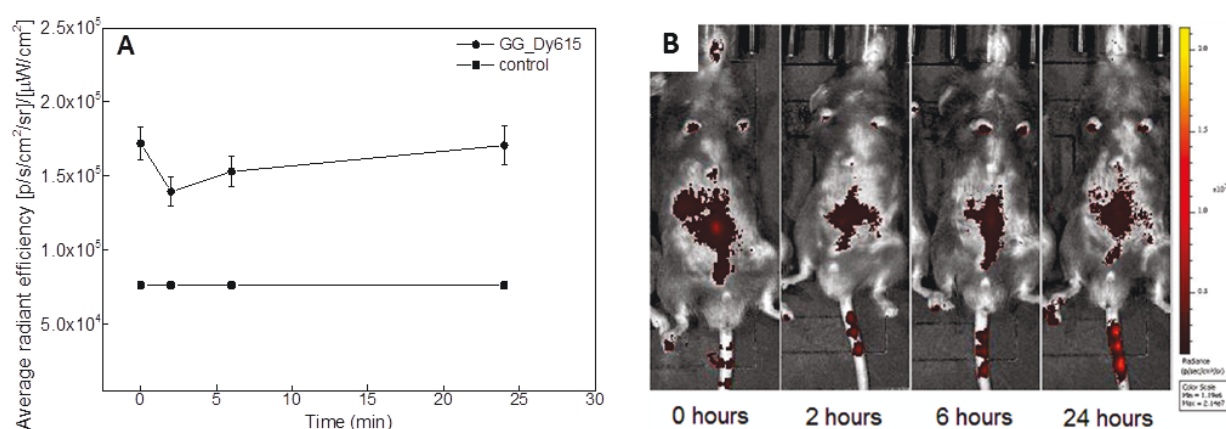


Figure 1. (A) The time dependence of fluorescence signals from the C57BL/6 mice after i.v. application of GG-Dy615 in comparison with the negative controls – the mice without application of GG-Dy615. (B) Example of fluorescence signal changes in the time from one mice after i.v. application of GG-Dy615.

Preliminary biological results indicated biocompatibility, biodegradability and non-toxicity of the prepared GG-based hybrid materials. Higher content of polyoxazoline chains in the synthesized materials slowed down cellular uptake. Low colocalization of the GG-based probes with lysosomes was observed, confirming that modified glycogen is degraded in the same way as the endogenous one.

The possibility of following the administrated nanoconjugates by both FLI and MRI techniques and successful results of our preliminary biological study on the GG-based materials encouraged us to perform another experiment on tumour-bearing rats. For this experiment two GG-based nanoconjugates were synthesized by the same approach mentioned

above with the only difference of using near infrared dye (IR800CW) instead of Dy615 to incorporate fluorescence label in the structure of polysaccharide derivatives. The prepared materials were denoted as GG_IR_DOTA-Gd and GG_POX_IR_DOTA-Gd for the one decorated with FL and MRI labels only and the one additionally grafted with POX chains, respectively. The content of IR dye was determined spectrophotometrically in water and was found to be 0.5 and 0.7 $\mu\text{mol/g}$ in the GG_IR_DOTA-Gd and GG_POX_IR_DOTA-Gd conjugates, respectively. The content of gadolinium in the final products was determined by inductively coupled plasma mass spectrometry and was found to be 0.26 and 0.2 mmol/g for GG_IR_DOTA-Gd and GG_POX_IR_DOTA-Gd, respectively.

In order to investigate the multi imaging properties of prepared GG-based conjugates carrying both FL and MRI contrast agents, *in vitro* experiment on phantoms was performed. Relaxivity of GG_IR_DOTA-Gd probe was higher compared to commercially available gadoterate meglumine (GM), although GG_POX_IR_DOTA-Gd exhibited lower values (Figure 2).

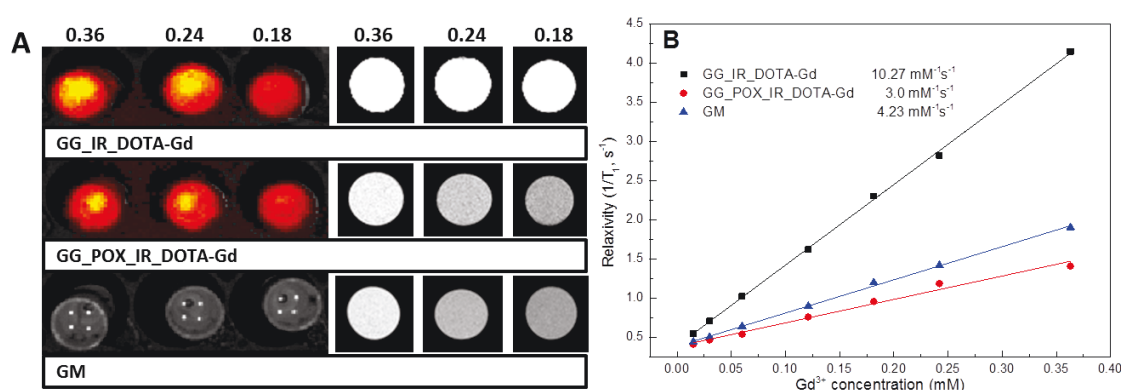


Figure 2. (A) Fluorescent and T_1 -weighted MR images of the glycogen-based probes without (GG_IR_DOTA-Gd) and with oxazoline (GG_POX_IR_DOTA-Gd) compared to gadoterate meglumine (GM). (B) Relaxivities r_1 of the tested probes measured at 0.5 T.

Tumours were induced in Rowett Nude (RNU) rats by subcutaneous injection of HUH7 cells (5×10^6) above the hind leg. After the intravenous administration, GG_IR_DOTA-Gd and GM were up taken by liver, although the amount of GG_POX_IR_DOTA-Gd in the organ was negligible. Increase of MR signal in liver and kidneys was higher for GG compared to GG_POX_IR_DOTA-Gd, however, the fluorescence signal of GG_POX_IR_DOTA-Gd was higher than those of GG_IR_DOTA-Gd. Visualized accumulation of all probes in tumour tissue can be seen in Figure 3A and what is important to highlight here, the contrast to noise ratio (CNR) from GG_IR_DOTA-Gd and GG_POX_IR_DOTA-Gd increased at day 7, while the signal of GM (0.02 mmol/kg) decreased (Figure 3B).

Therefore, the obtained results revealed suitable properties of the novel glycogen-based compounds for nanomedical application, including the tumour-targeting character. The MR signal increment in tumours was long-lasting with the higher contrast increase of GG_IR_DOTA-Gd and GG_POX_IR_DOTA-Gd compared to GM, suggesting continuous accumulation by enhanced permeability and retention (EPR) effect. The modification with polyoxazoline chains resulted in slower elimination rate of the GG_POX_IR_DOTA-Gd that increased probability of accumulation in the tumour tissue by low uptake of GG_POX_IR_DOTA-Gd into organs compared to GG_IR_DOTA-Gd. The obtained results confirmed a high potential of the prepared probes for tumour diagnosis and treatment.

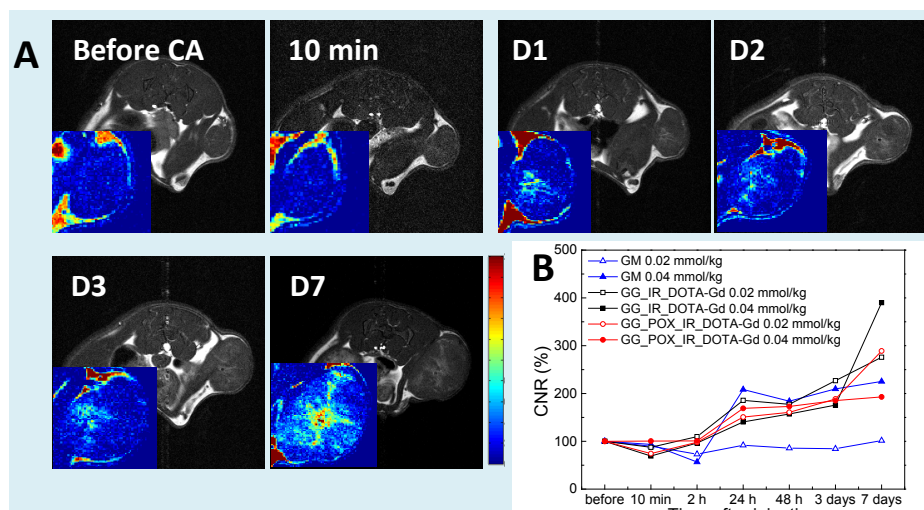


Figure 3. (A) MR images and corresponding CNR maps (inserts) values of tumour tissue after administration of glycogen-based probes; (B) Calculated CNR values of tumours at various time points after injection of the glycogen-based probes and GM.

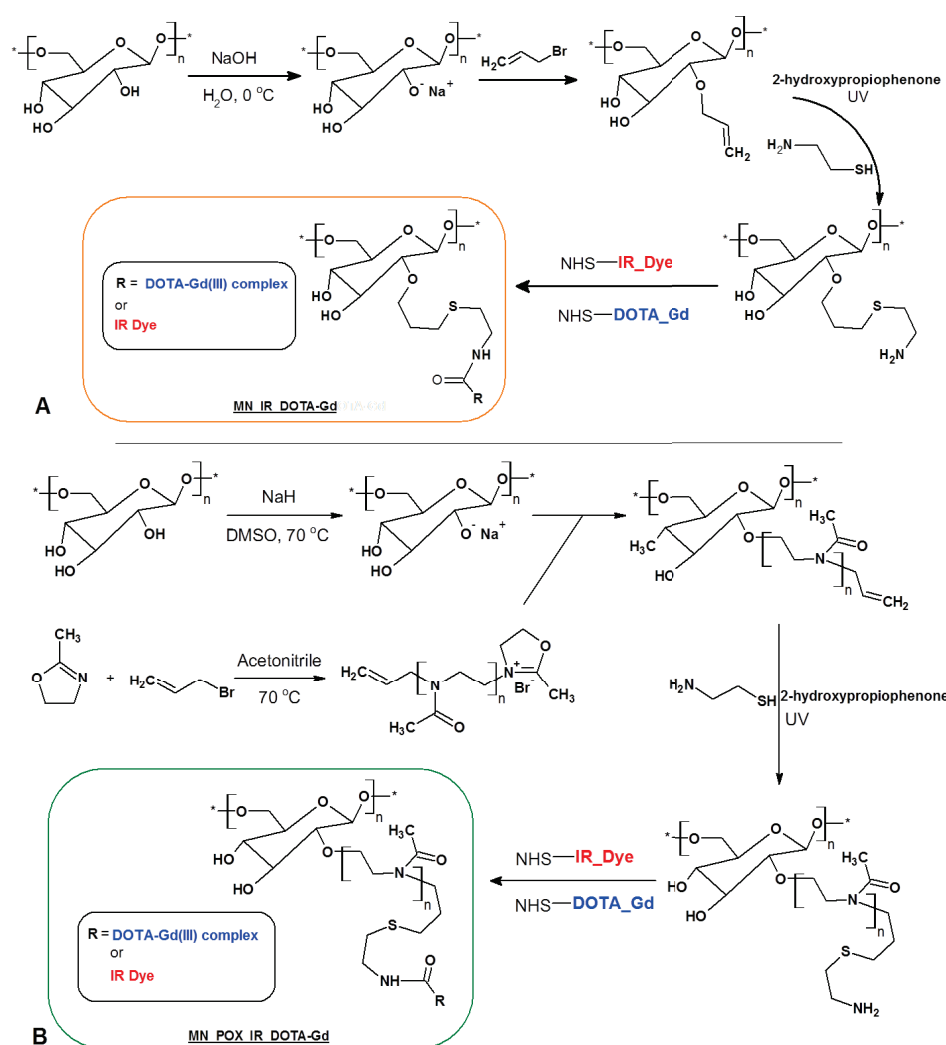
3.1.2. Mannan-based conjugates for multimodal imaging

During this work, the natural biodegradable polysaccharide mannan (MN) was modified in two different ways to obtain conjugates bearing a fluorescent label and a MRI contrast probe. The first approach was devoted to the synthesis of polysaccharide-based conjugate without POX in the structure (Scheme 2A). The modification procedure was started by alkylation reaction of commercial mannan (from *Saccharomyces cerevisiae*) with allyl bromide followed with the thiol-ene click chemistry reaction with cysteamine, using 2-hydroxy-2-methylpropiophenone as an initiator under UV irradiation. The obtained primary amino groups containing mannan was then conjugated with *N*-hydroxysuccinimide (NHS) esters of infrared dye (IR800CW) and 1,4,7,10-tetraazacyclododecane-1,4,7,10-tetraacetic acid (DOTA) chelator. Finally, the product was subjected to react with gadolinium (III) chloride to chelate Gd^{3+} ions, resulting in the mannan-based conjugate with the fluorescence and MR imaging labels, denoted as MN_IR_DOTA-Gd.

The second synthetic path was focused on the preparation of mannan-based conjugate with grafted POX chains (Scheme 2B), which would prolong the biodegradation of the final hybrid structure compared to the MN_IR_DOTA-Gd (without POX in the structure). This modification procedure starts from the formation of mannan sodium alkoxide in anhydrous DMSO and accomplished by reaction of the last one with active POX chains, which were obtained by cationic ring-opening polymerization (CROP) in anhydrous acetonitrile. As a result, mannan-graft-poly(2-methyl-2-oxazoline) (denoted as MN_POX) with grafting density 1 graft per 5 glucose units was obtained. The molecular weight of POX grafts was determined by mass spectrometry after termination of active chains with water: number-average molecular weight $M_n = 870$ g/mol, polydispersity $D = M_w/M_n = 1.14$, where M_w is the weight-average molecular weight. Because polymerization of 2-methyl-2-oxazoline was initiated with allyl bromide, grafted POX chains have a double bond at the end. In order to introduce the FLI and MRI labels, this vinyl containing mannan derivative was then modified by the same procedure as for MN_IR_DOTA-Gd: introduction of primary amino groups by thiol-ene “click” reaction followed by complexation with the corresponding NHS esters. The amount of IR dye was determined spectrophotometrically in water and was found to be 0.72 and 0.66 $\mu\text{mol/g}$ in the MN_IR_DOTA-Gd and MN_POX_IR_DOTA-Gd conjugates, respectively. The content of gadolinium in the final products was determined by inductively coupled

plasma mass spectrometry and was found to be 0.252 and 0.26 mmol/g for MN_IR_DOTA-Gd and MN_POX_IR_DOTA-Gd, respectively.

In order to characterize the aqueous solution behaviour of the prepared MN-based conjugates, dynamic light scattering measurements were conducted. To investigate the difference in D_{hyd} after mannan modification, both hybrid systems were dissolved in water and PBS at concentration 1 mg/mL and compared to the same solutions of neat mannan (Table 2). The size distributions of neat and modified MN indicate the increase in hydrodynamic diameter. In aqueous solution, the D_{hyd} of both MN_IR_DOTA-Gd and MN_POX_IR_DOTA-Gd were *ca.* two times larger (~ 6 nm) than native MN (2.4 nm). Also, in order to determine the ZP of the nanostructures formed by MN derivatives, the electrophoretic mobility measurements were done on the same solutions as for DLS. The small negative value of ZP in case of MN_IR_DOTA-Gd compared to the neat mannan, which had a ZP around 0 mV, confirms the presence of carboxylate groups in the structure of MN-based contrast agents, originating from FL and MR labels (Table 2).



Scheme 2. Synthesis paths for mannan modification: preparation of (A) MN_IR_DOTA-Gd and (B) MN_POX_IR_DOTA-Gd.

In the case of MN_POX_IR_DOTA-Gd, the presence of grafted POX chains led to a slight increase of ZP up to 2.9 mV compare to the neutral character of the neat MN (Table 2). No substantive difference in hydrodynamic diameter was observed when using PBS (pH 7.4) as a solvent for the investigated compounds. The values of D_{hyd} for neat MN as well as for

two prepared conjugates were ~ 7 nm (Table 2). However, the ZP of all three samples in PBS was small and negative, which can be explained by a formation of counter ion layer (Table 2).

Table 2. Hydrodynamic diameter and ζ -potential of the final MN-based conjugates obtained by DLS and electrophoretic mobility measurements, respectively.

Sample	D_{hvd} , nm		ζ -potential, mV	
	PBS	H ₂ O	PBS	H ₂ O
Mannan ^a	7.2	2.4	-5.6	0.2
MN_IR_DOTA-Gd	6.6	6.2	-11.5	-4.0
MN_POX_IR_DOTA-Gd	7.2	6.0	-6.7	2.9

^a– commercial (native) mannan from *Saccharomyces cerevisiae*

The imaging properties of the prepared conjugates were analysed with the help of *in vitro* experiment on phantoms. Both mannan-based agents showed higher r_1 and r_2 relaxivities than the commercially available GM, while relaxivities of MN_IR_DOTA-Gd and MN_POX_IR_DOTA-Gd were comparable. Also MR signal and corresponding CNR values of MN-based probes were higher compared to GM (Figure 4A, C).

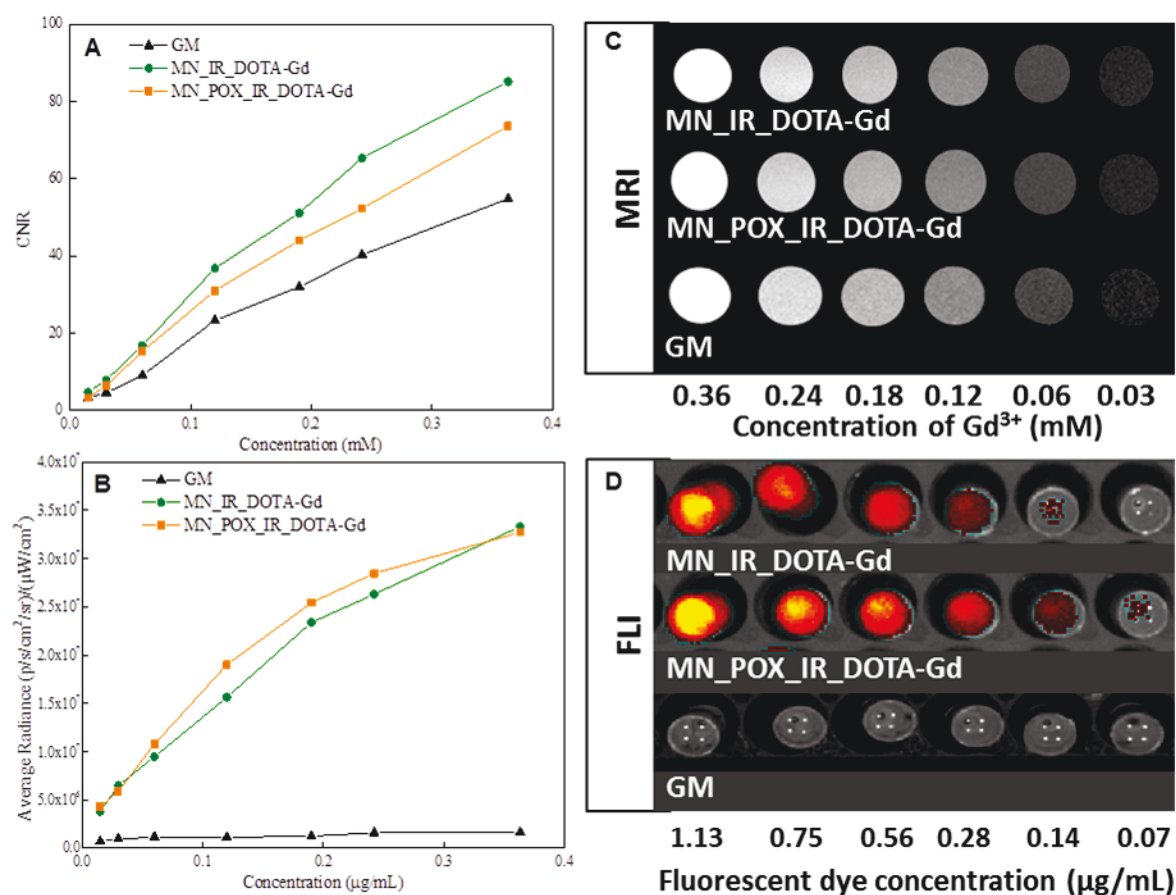


Figure 4. (A) The MRI and FLI signals of the MN_IR_DOTA-Gd, MN_POX_IR_DOTA-Gd and GM. CNR calculated from MR images and (B) fluorescence signal of the probes of various concentration of Gd³⁺ or fluorescence dye. (C) Representative MR images of the probes with different Gd³⁺ concentration – the numbers represents Gd³⁺ concentration expressed in mM; (D) the FLI images of the probes with different dye concentration; the numbers represents concentration of a fluorescent dye expressed in $\mu\text{g/mL}$.

After intramuscular administration to the animals, both MN_IR_DOTA-Gd and MN_POX_IR_DOTA-Gd agents were visualized at the injection sites by MRI and FLI techniques for 21 days. The fluorescence signal of MN_POX_IR_DOTA-Gd in muscle (the site of injection) was higher compared to MN_IR_DOTA-Gd within the first two days after the probes administration, showing a prolongation of imaging window due to poly(2-methyl-2-oxazoline) conjugation and proving a slower biodegradation of the conjugate (Figure 5).

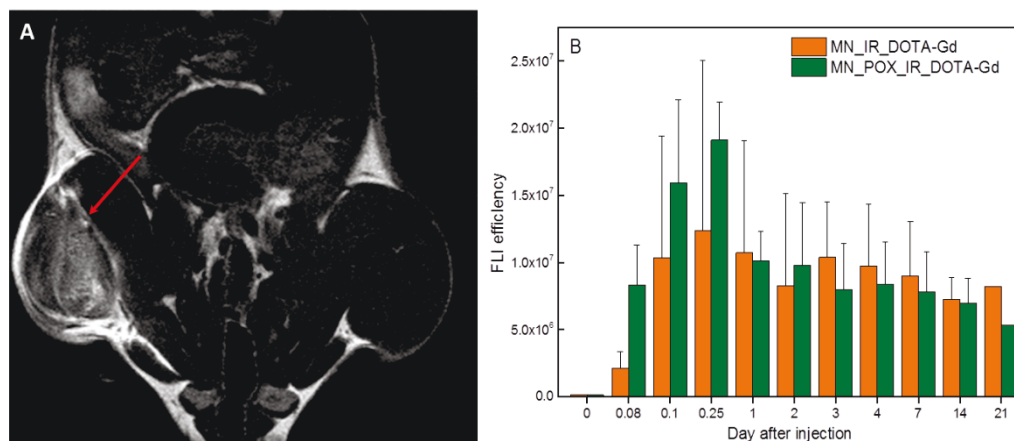


Figure 5. (A) The representative T₁-weighted MRI image of a mouse with injected MN_IR_DOTA-Gd probe into the hind leg; the arrow points the injection site. (B) The time course of fluorescence signal from the injection site (muscle).

In addition, the first day after the probes administration the higher FLI signal in the liver was visualized from MN_IR_DOTA-Gd compared to MN_POX_IR_DOTA-Gd, and this trend persisted through the whole examination time (Figure 6A, C). During the first day after probes administration, higher FLI and MRI signals from the lymph nodes were detected in case of MN_IR_DOTA-Gd confirming its faster degradation (Figure 6B).

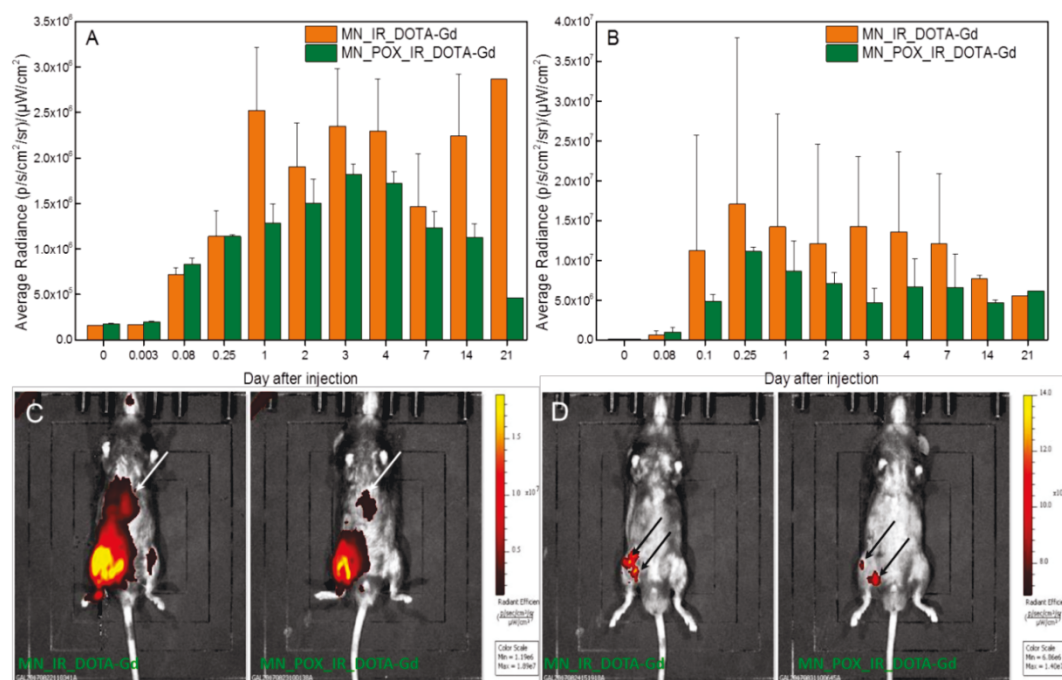


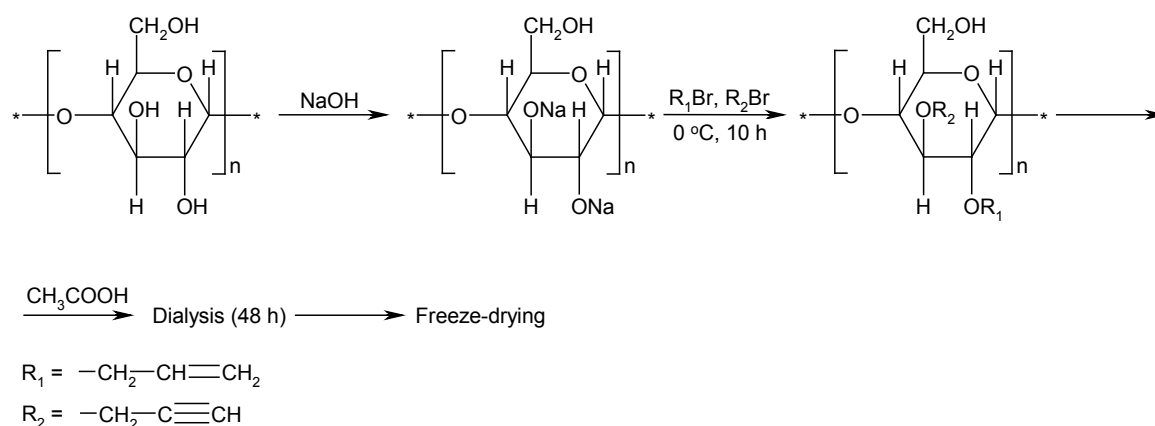
Figure 6. Time course of *in vivo* fluorescence signal originating from the liver (A) and the lymph nodes (B). Representative fluorescence images of mice after injection with MN_IR_DOTA-Gd and MN_POX_IR_DOTA-Gd (C, D). The arrows mark liver (C) and lymph nodes (D).

After sacrifice of experimental animals, *ex vivo* fluorescence imaging of the harvested organs also confirmed lower accumulation of MN_POX_IR_DOTA-Gd in the liver, spleen and kidneys for all time intervals. The signals originating from the lymph nodes were comparable for both MN_IR_DOTA-Gd and MN_POX_IR_DOTA-Gd conjugates within 7, 14 and 21 days after the probe administration and remained similar during the whole examination time. On the other hand, signal from organs (liver, spleen, kidneys) continuously decreased within time for both conjugates, demonstrating gradual biodegradation of mannan probes *in vivo*.

The prepared mannan-based conjugates were shown to possess superior properties compared to the commercially available contrast agent GM including MR relaxivity and possibility of fluorescence imaging. Visualized accumulation of the agents in the lymph nodes confirmed its immune-targeted property and possible use of them in metastasis diagnostic. Moreover, the possibility of further modification for incorporation of specific drugs makes these structures promising candidates for nanomedicine application.

3.2. Glycogen-based fibrous material for tissue engineering

The allylated and propargylated glycogen (denoted as APG) was prepared by alkylation reaction of hydroxyl groups in the GG structure with the mixture of allyl and propargyl bromides in alkaline aqueous solution (Scheme 3). The presence of both double and triple bonds in APG structure allowed us to perform further modification of the material by functionalization *via* triple and crosslinking *via* double bonds in the same time. The degree of GG adjustment with allyl groups should be high enough to obtain a sufficiently crosslinked, water-insoluble material. According to our previous experiments (data not shown), when more than 36% of the hydroxyl groups in its structure are substituted with alkyl, glycogen becomes water insoluble. Additionally, because of the strong influence of functionalization degree on the rate of polysaccharides biodegradation, exceeding a specific value of functionalization can result in substantial decrease of enzymatic hydrolysis rate²⁰. Therefore, the modification of the native GG was performed in a way to obtain APG with 15% of allyl and 5% of propargyl group substitution per D-glucose unit (calculated from ¹H NMR spectra). Resulting GG-based derivate was used for the preparation of different 3D structures *via* freeze-drying, where morphology of the final material depends on the initial concentration of APG aqueous solution²². In this thesis 0.5 and 5.0 wt. % aqueous solutions of APG (denoted as APG-0.5 and APG-5, respectively) were used for the preparation of scaffolds.



Scheme 3. The modification procedure for GG allyl and propargyl derivatives preparation.

The scanning electron microscopy (SEM) micrographs of the GG-based freeze-dried materials show microfibers and sponge-like structures fabricated from 0.5 (Figure 7A) and 5.0 wt. % (Figure 7B) aqueous solutions of APG, respectively. In the case of using APG-0.5

solution, the fibres with an average size of approximately 2.5 μm in diameter were formed, while lyophilisation of the APG-5 solution led to formation of sponge-like structures. In both cases the obtained materials were highly porous with fully interconnected pores.

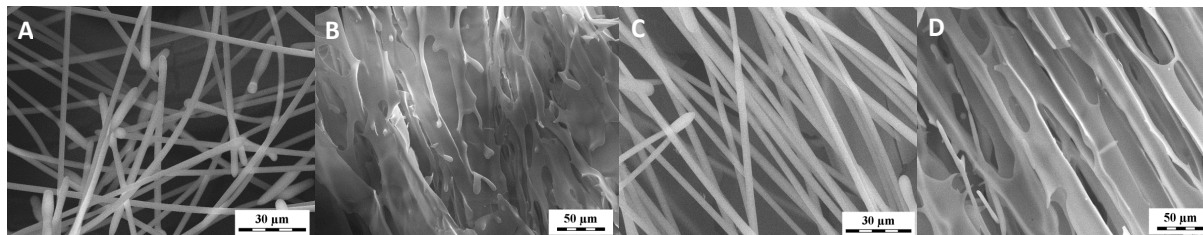


Figure 7. SEM micrographs of freeze-dried (A) APG-0.5, (B) APG-5 and after β -irradiation (C) APG-0.5 and (D) APG-5 materials.

Insolubility in water is an essential feature for any material to be used in tissue engineering (TE) as a scaffold. Thus, presence of the double bonds in the allyl groups of APG was used to perform crosslinking. As a source of electron radiation the Microtron MT25 accelerator with a high frequency source was used (experiments were conducted at Nuclear Physics Institute of the ASCR). The used microtron provides the incident electron beam (10 MeV, 25 μA , 2 kGy/min) that caused radically initiated crosslinking of APG samples. The fibrous structures from GG derivatives were exposed to different radiation doses in the range of 2-150 kGy. For the preparation of crosslinked GG-based material for tissue engineering purposes the radiation dose of 2 kGy was established as an optimal one.

The obtained SEM micrographs of the irradiated APG-0.5 and APG-5 samples (Figure 7C, D) revealed no significant changes in the structure of materials compared to the non-irradiated ones.

The biocompatibility of newly prepared GG-based materials and their interactions with living cells were studied *in vitro* with human osteoblast-like MG 63 cell line that was used as a model of bone tissue. The cell spreading area was significantly larger on the control PS dish compared to the tested GG sample for the whole investigation period (Table 3). Although, the presence of APG-0.5 sample in culture decreased the proliferation of MG 63 cells, the morphology of the cells remained unchanged and they were distributed homogeneously on the bottom of the dish. In addition, the number of cells increased continuously during the cultivation time and on 7th day of experiment its merging layer was created (Table 3).

Table 3. The adhered cells and spreading area of human osteoblast-like MG 63 cells on the 1st, 3rd and 7th day after seeding on control polystyrene (PS), APG-0.5, APG-5, RGD-APG-0.5 and RGD-APG-5 materials; grey colour denotes data from experiment with the glycogen materials modified with RGD peptide.

Material	Adhered cells, x 10 ² cells/cm ²		
	1 st day	3 rd day	7 th day
PS	101 ± 20	426 ± 30	162 ± 17
APG-0.5	69 ± 17	165 ± 35	516 ± 17
PS	195 ± 44	323 ± 30	1315 ± 59
RGD-APG-0.5	254 ± 26	435 ± 67	1471 ± 104
RGD-APG-5	230 ± 21	354 ± 49	1310 ± 130

As it was mentioned above, the presence of triple bonds provides a possibility for additional functionalization of the material with some active moiety. In this thesis, the

modification of GG derivatives was done with azidopentanoic-GGGRGDSGGGY(¹²⁵I)-NH₂ peptide (RGD) *via* copper-catalyzed alkyne-azide cycloaddition. Biological testing of resulting materials, denoted as RGD-APG-0.5 and RGD-APG-5 for 0.5 and 5.0 wt. % aqueous solutions, respectively, was conducted with the same cell line. In contrast to the first *in vitro* experiment, the population densities of cells cultivated with RGD-APG samples were higher than in polystyrene control dishes for RGD-APG-0.5 and comparable in case of RGD-APG-5 (Figure 8, Table 3). Again, the number of osteoblast-like cells increased continuously during the investigated time and at the end of experiment and the confluent layer of cultivated cells was created (Figure 8C and F).

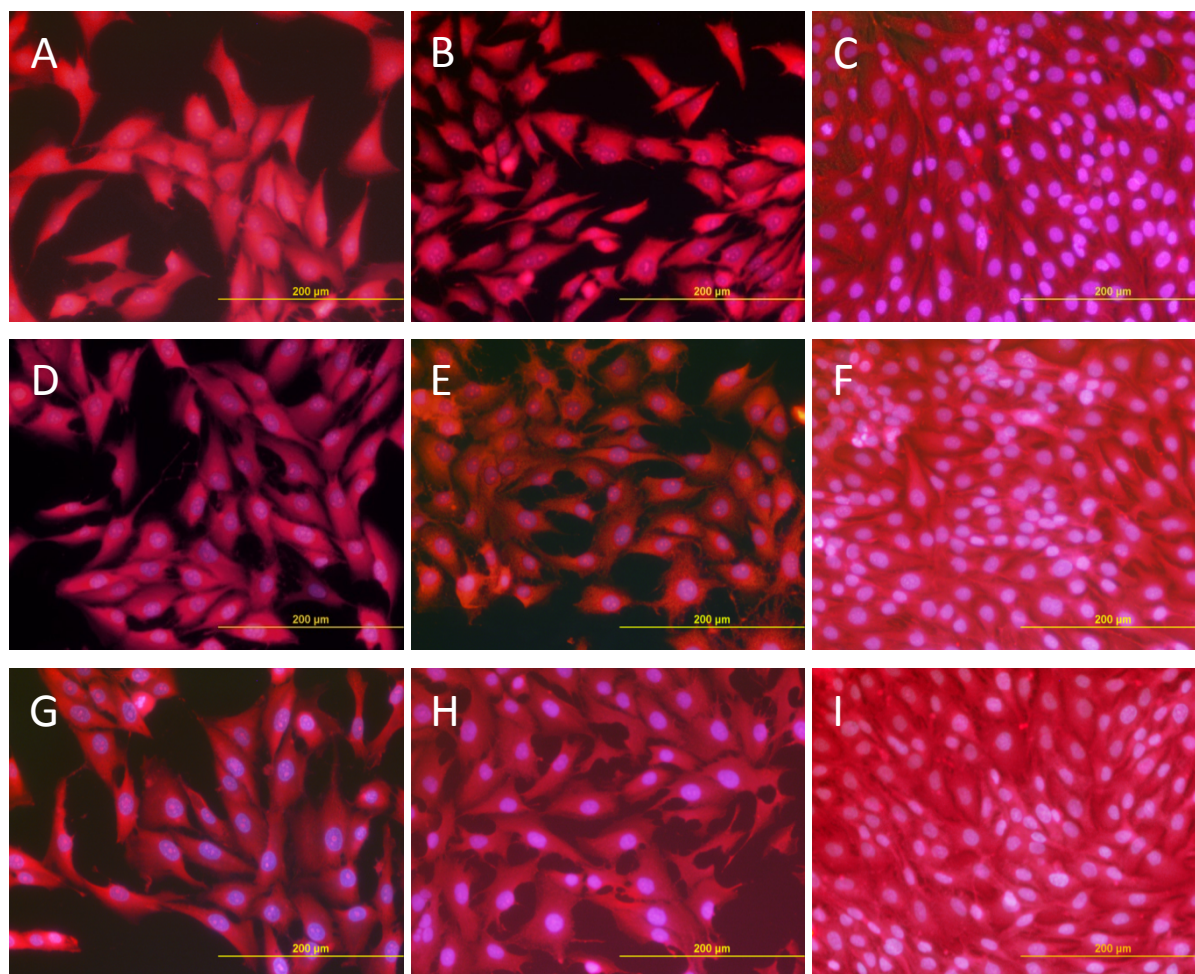


Figure 8. Morphology of human osteoblast-like MG 63 cells on (A, D, G) day 1, (B, E, H) day 3 and (C, F, I) – day 7, after seeding on a control polystyrene dish (G, H, I) or on the bottom of a cultivation dish with RGD-APG-0.5 (A, B, C) or RGD-APG-5 (D, E, F). The cells were stained with Texas Red C2-maleimide and Hoechst #33342. Olympus IX 50 microscope and Olympus DP 70 digital camera; obj. 20x, bar = 200 μm.

Therefore, the obtained results showed that the cells growing in the presence of GG-based materials behaved physiologically without any signs of the cell damage. The preliminary biological investigations confirmed the possibility of using such systems as wound healing dressings and proved the beneficial effect of peptide on the cell growth.

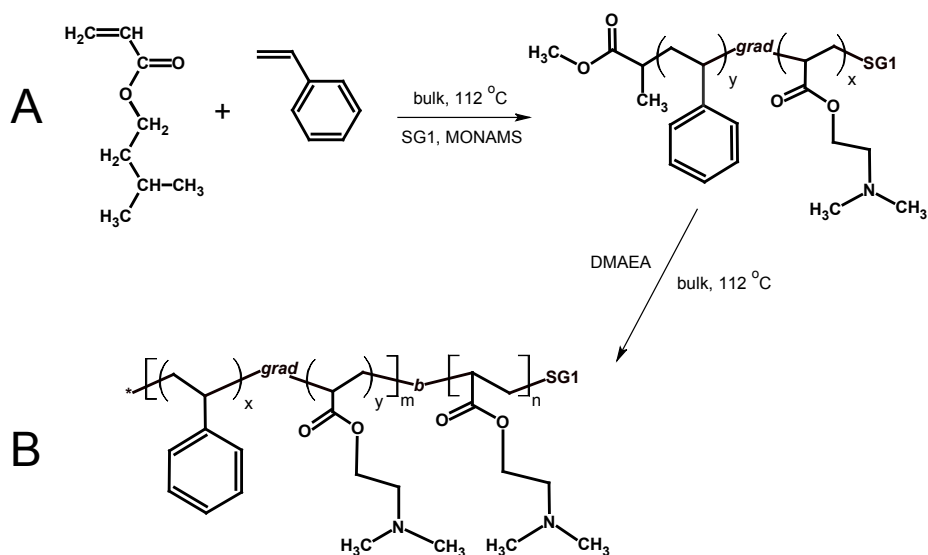
3.3. Synthesis of amphiphilic block copolymers and their modification

Currently, a continuously increasing interest is devoted to the nanostructures assembled from amphiphilic polycations as non-viral gene delivery systems²³. Among the

variety of polyelectrolytes used as gene carriers, poly(2-dimethylaminoethyl methacrylate) (PDMAEMA) was widely studied²⁴⁻²⁶. However only few recent works are dedicated to preparation and investigation of new polymer systems based on its homologue – poly(2-dimethylaminoethyl acrylate) (DMAEA). In this thesis, the novel pH- and thermo-responsive amphiphilic diblock copolymers, comprising an hydrophilic poly(2-dimethylaminoethyl acrylate) (PDMAEA) block and an amphiphilic poly(styrene-*grad*-2-dimethylaminoethyl acrylate) (P(S-*grad*-DMAEA)) block were synthesized.

Because reactivity ratios of styrene (S) and DMAEA monomer mixture have not been studied yet, we started the synthesis of designed amphiphiles with the investigation of their reactivity ratios using ¹H NMR spectroscopy.

The experiments were conducted using five initial mixtures with the different feed composition of S and DMAEA containing 20, 40, 50, 60 and 80 mol. % of S ($f_s = 0.2, 0.4, 0.5, 0.6$ and 0.8), with a targeting degree of polymerization of 100. The kinetics of performed nitroxide-mediated radical polymerization (NMRP), using MONAMS as initiator and SG1 as a control agent, was followed by ¹H NMR (Scheme 4A). The polymerizations were performed in a bulk at 112 °C and were stopped at 50-70 % of monomers conversion.



Scheme 4. Synthetic procedure and chemical structure of the S and DMAEA copolymers prepared by NMRP.

The monomer reactivity ratios of copolymerization initiated by MONAMS were determined with different methods, such as Mayo-Lewis²⁷, Kelen-Tüdös²⁸, nonlinear least-squares²⁹ and Skeist³⁰, and were found to be $r_S = 1.16$ and $r_{DMAEA} = 0.25$. The results reveal that styrene is much more reactive than DMAEA and the formation of spontaneous gradient copolymer, with increasing amount of DMAEA within a chain length (P(S-*grad*-DMAEA)), is expected.

Based on the obtained reactivity ratios of the comonomers S and DMAEA, spontaneous block-gradient P(S-*grad*-DMAEA) (named GX, with X the molar fraction of DMAEA in the copolymer) should be obtained using a batch copolymerization. This time, two different molar compositions of the resulting copolymers were targeted – $F_{DMAEA} = 50$ and $F_{DMAEA} = 30$, which were denoted as G50 and G30, respectively. The kinetic plots of performed NMRP (from ¹H NMR) with two different initial monomeric mixtures are represented in Figure 9. As one can see, the relationships of $\ln([M]_0/[M])$ versus time are linear within the whole reaction time, confirming well-controlled polymerization. Moreover, the experimental molar masses of the series of P(S-*grad*-DMAEA) copolymers increase linearly with the overall monomer conversion (Figure 10A for G50). The number average

molecular weight is proportional to conversion, and the slope is approximately the same as in the theoretical curve, although the values of M_n are slightly bigger than the theoretical ones. Moreover, the decrease of dispersity and the shift of the SEC chromatograms towards low elution volumes throughout the copolymerization (Figure 10B for G50) support the controlled character of the bulk NMRP copolymerization.

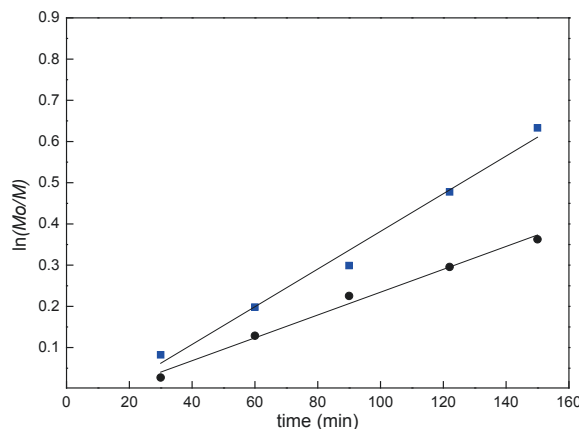


Figure 9. Kinetic plot of $\ln\left(\frac{[M]_0}{[M]}\right)$ versus time for a bulk NMP copolymerization of DMAEA and S at 112°C with the initial feed composition of DMAEA (f_{DMAEA}) of 55 mol. % (■) and 30 mol. % (●). The lines correspond to the linear regression.

The obtained gradient copolymers were further successfully used to initiate a homopolymerization of DMAEA as a second block using again NMRP (Scheme 4B). The resulting two amphiphilic diblock copolymers of structure $P(S_{0.5}\text{-grad-DMAEA}_{0.5})_{70}\text{-}b\text{-}P(\text{DMAEA})_{50}$ and $P(S_{0.7}\text{-grad-DMAEA}_{0.3})_{70}\text{-}b\text{-}P(\text{DMAEA})_{40}$ were denoted as DG50 and DG30, respectively, and their self-assembly in aqueous solutions as well as influence of pH, ionic strength and temperature on the formation of nanoaggregates were studied.

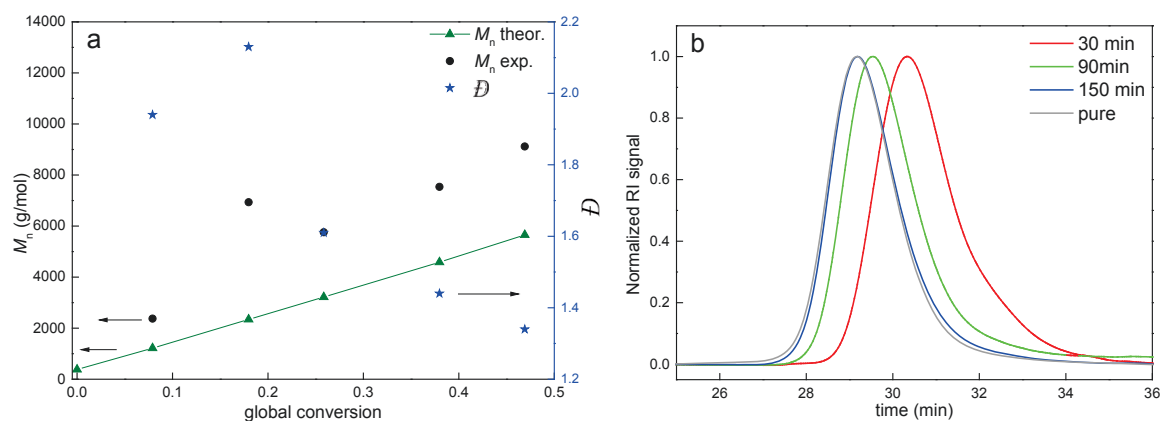


Figure 10. (A) The evolution of M_n and M_w/M_n with conversion for performed NMRP of $P(S_{0.5}\text{-grad-DMAEA}_{0.5})_{70}$ (G50) and (B) the SEC elution curves of $p(\text{DMAEA-grad-S})$ copolymer with DMAEA/S ratio 50/50 (G50) from a viscosity detector (using universal calibration analysis).

The self-assembling behaviour of the copolymers under different pH was then investigated using DLS technique. Experiments were conducted using an auto-titration set-up, which allowed to simultaneously change pH of solution and to measure the corresponding hydrodynamic diameter (D_{hyd}) of the created nanostructures (Figure 11).

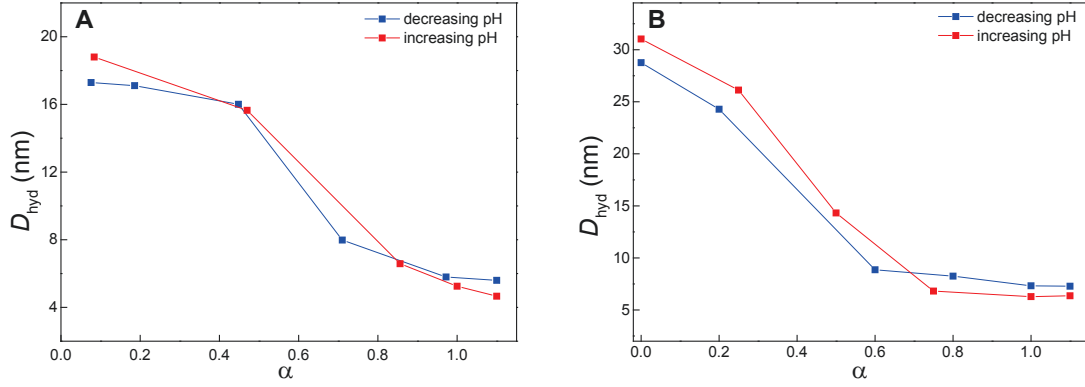


Figure 11. (A) DLS titration curves for aqueous solution of block-gradient copolymer P(S_{0.5-grad}-DMAEA_{0.5})_{70-b}-PDMAEA₅₀ (DG50) and (B) P(S_{0.7-grad}-DMAEA_{0.3})_{70-b}-PDMAEA₄₀ (DG30) at concentration 0.1 wt. %.

Aggregates of about 20 nm for DG50 and 30 nm for DG30 are formed at low ionization degree (around pH 8). When the ionization degree increases, strong electrostatic repulsion between charges along the polymer backbone are generated, resulting in the dissociation of the aggregates to single polymer chains, which is confirmed by the low value of D_{hyd} at high α values ($D_{\text{hyd}} \sim 5$ nm). We assumed that the formed spherical aggregates correspond to micelle-like structures comprising a hydrophobic P(S-*grad*-DMAEA) core and a hydrophilic PDMAEA shell. When decreasing α , the transition region, where the self-assembly occurs, corresponds to pH ~ 7 and 5 for DG50 and DG30, respectively. This difference can be explained by a higher fraction of styrene in the associating block for DG30 (70 mol. % of styrene) compared to DG50 (50 mol. % of styrene), which render the dissociation of the aggregates into unimers with increasing α more difficult. Remarkably, the pH-controlled self-assembly of the copolymers is reversible. When the solutions are brought back to $\alpha = 100\%$, the DLS titration curves overlay (Figure 11).

For deeper characterization of the self-assembling behaviour of the diblocks in the aqueous solution small angle neutron scattering (SANS) experiments were conducted on the copolymers dispersed in D₂O at different α values. An adjustment of targeted α values was done by adding concentrated solutions of NaOD (40 wt. %) or DCl (35 wt. %) in deuterium oxide. The obtained SANS data are shown in Figure 12.

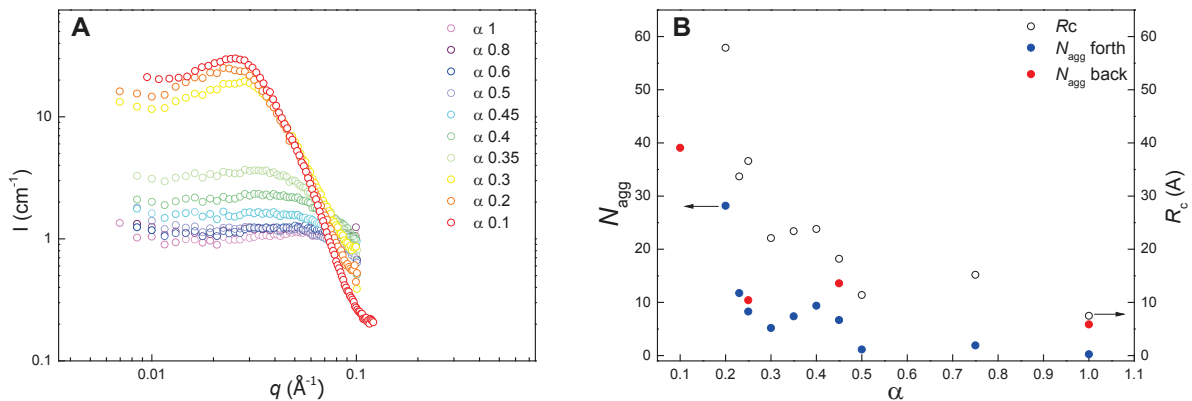
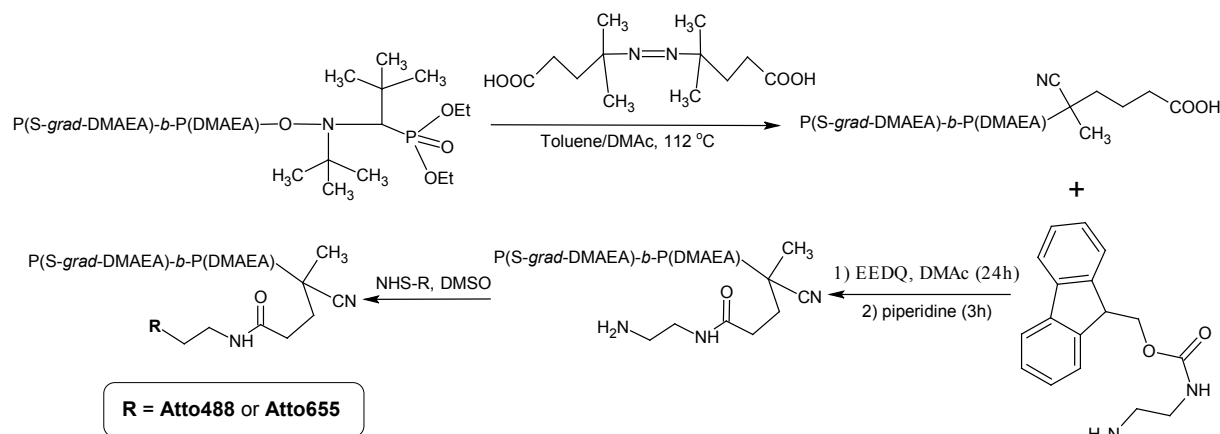


Figure 12. (A) Scattering intensity (I) as a function of scattering wave vector (q) at different ionisation degrees and (B) evolution of the aggregation number (N_{agg} , full symbol) and core radius of micelles (R_c , empty symbol) as function of ionisation degree α for DG50 (P(S_{0.5-grad}-DMAEA_{0.5})_{70-b}-P(DMAEA)₅₀) block-gradient copolymers solutions in deuterium oxide at concentration 10 wt. %.

The synthesized copolymer DG50 was further modified *via* typical peptide chemistry approach (Scheme 5) in order to obtain a primary amino group containing polymer. This primary amino groups-terminated polymer was then labelled with fluorescent dyes Atto488 or Atto655 as the corresponding NHS esters, resulting in the functionalized amphiphilic diblock copolymers for preliminary biological tests as a model of self-assembled stimuli-sensitive nanostructures, denoted as DG50-488 and DG50-655, respectively.



Scheme 5. Modification procedure for DG50 amphiphilic copolymer.

Cytotoxicity of the modified diblock copolymer was studied on HeLa and primary fibroblast cell lines. The *in vitro* viability of both tested cell types did not possess significant difference after incubation with the prepared diblock copolymers, revealing non-toxicity of the obtained materials. There was only a small decrease in viability of fibroblasts at quite high concentration of both DG50-488 and DG40-655 copolymers. The biocompatibility test revealed a possibility of using these materials as a perspective drug- or gene delivery systems.

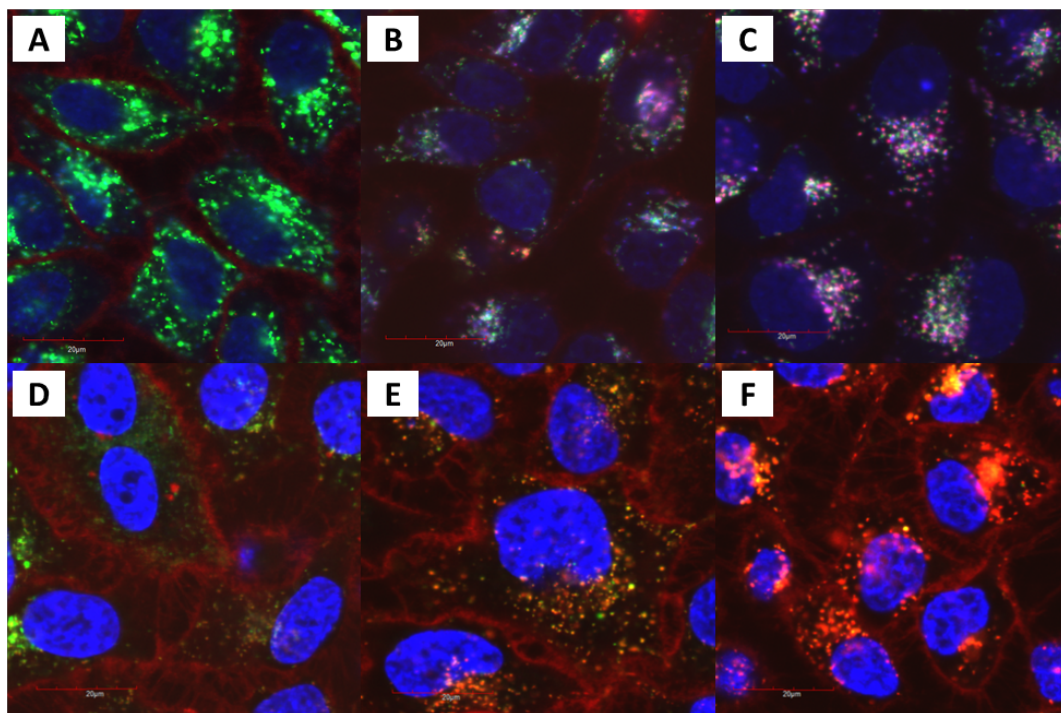


Figure 13. The intracellular tracking of (A, B, C) DG50-488 and (D, E, F) DG50-655 polymers. The cells were incubated with polymer for 2 (A, D), 6 (B, E) and 24 (C, F) hours before LSCM. Lysosomes were stained by LysoTracker Yellow (coloured green), the nuclei were stained by Hoechst 33342 (coloured blue) and polymers are coloured red.

Laser scanning confocal microscopy (LSCM) was used for the evaluation of intracellular tracking of fluorescence labelled polymers and their colocalization with lysosomes. The obtained results from confocal microscopy studies, represented on the Figure 13, show that the labelled copolymer is located in the cell membrane after 2 h of incubation (Figure 13A, D). However, because of the cationic character of the copolymer, within time it is able to internalize and accumulate into the lysosomes (Figure 13B, C). Interestingly, the behaviour of the two labelled polymers was not identical. Despite the low amount of labels in the copolymers they play an important role in the localization of nanostructures *in vitro*. Thus, after 24 h of cell incubation with the functionalized polymers, DG50-488 micelles were localized mainly inside lysosomes, while micelles from DG50-655 were present both on the cell membrane surface and in the lysosomes. The possible reason for such difference can be the more cationic character of Atto655 label compared to Atto488. Therefore, for design and preparation of novel nanoagents for biomedicine, not only a proper polymer but also a specific label for its functionalization have to be carefully considered.

4. Conclusions

- Natural polysaccharide glycogen (GG) was successfully modified in order to obtain the novel hybrid nanostructures for drug delivery and diagnostic purposes. Grafting of polysaccharide structure with the biocompatible poly(2-methyl-2-oxazoline) chains was performed in order to tune the biodegradation process. The prepared GG-based hybrid systems were functionalized with both fluorescence and magnetic resonance imaging agents, which allows following the fate of the administrated compounds simultaneously by different techniques. Intracellular localization, cytotoxicity and internalization route of modified glycogen derivatives were examined on HepG2 cell line, while biodistribution of the obtained hybrid materials was investigated by *in vivo* fluorescence imaging using C57BL/6 mice. The biological tests prove biocompatibility, non-toxicity and biodegradability of the prepared GG-based hybrid systems. Moreover, externally administrated modified glycogen has been shown to degrade the same way as an endogenous one.
- An easy synthetic approach was used for modification of another natural polysaccharide – mannan (MN) in order to obtain novel hybrid systems as multimodal imaging probes for diagnostic purposes. The obtained mannan-based conjugates contained both fluorescence IR dye and Gd³⁺ MRI contrast agent in the structure and possessed sufficient sensitivity for *in vivo* fluorescence imaging and superior MR properties compared to a commercial contrast agent. Visualized accumulation of the agents in the lymph nodes confirmed the immune-targeted property of the newly prepared polysaccharide-based conjugates and possible use of them in metastasis diagnostics.
- Modified glycogen was used to prepare fibrous and sponge-like structure by simple “green” method for regenerative tissue engineering purposes. Electron beam processing of obtained architectures provided cross-linked, water-insoluble materials. Biological investigation of the prepared systems proved its non-toxicity and beneficial effect on the growth of adjacent cells.
- Amphiphilic diblock copolymers of S and DMAEA with a gradient structure of associating block were synthesized using nitroxide-mediated controlled radical polymerization. Characterization of their behaviour in aqueous solutions and results from preliminary biological test proved their potential as nanocarriers for bioactive cargo delivery.

5. References

1. D.A. Vanden Bout, Metal nanoparticles: synthesis, characterization, and application, Ed. by D.L. Feldheim and C. A. Foss Jr., Marcel Dekker, New York, US, 2002.
2. J.F. Hicks, F.P. Zamborini and R.W. Murray, Dynamics of electron transfers between electrodes and monolayers of nanoparticles, *J. Phys. Chem. B*, 2002, 106, 7751–7757.
3. W. Chen, D. Grouquist and J. Roark, Voltage tunable electroluminescence of CdTe nanoparticle light-emitting diodes, *J. Nanosci. Nanotechnol.*, 2002, 2, 47–53.
4. H. Boulaiz, P.J. Alvarez, A. Ramirez, J.A. Marchal, J. Prados, F. Rodriguez-Serrano, M. Peran, C. Melguizo and A. Aranega, Nanomedicine: application areas and development prospects, *Int. J. Mol. Sci.*, 2011, 12(5), 3303–3321.
5. D. Dheer, D. Arora, S. Jaglan, R.K. Rawal and R. Shankar, Polysaccharides based nanomaterials for targeted anti-cancer drug delivery, *Journal of Drug Targeting*, 2017, 25(1), 1–16.
6. J.M. Myrick, V.K. Vendra and S. Krishnan, Self-assembled polysaccharides nanostructures for controlled release applications, *Nanotechnol. Rev.*, 2014, 3(4), 319–346.
7. X.X. Xi, M. Wang, Y. Lin, Q. Xu and D.L. Kaplan, Hydrophobic drug-triggered self-assembly of nanoparticles from silk-elastin-like protein polymers for drug delivery, *Biomacromolecules*, 2014, 15(3), 908–914.
8. F. Chiellini, A.M. Piras, C. Errico and E. Chellini, Micro/nanostructured polymeric systems for biomedical and pharmaceutical applications, *Nanomedicine*, 2008, 3(3), 367–393.
9. M. Delbianco, P. Bharate, S. Valera-Aramburu and P.H. Seeberger, Carbohydrates in supramolecular chemistry, *Chem. Rev.*, 2016, 116(4), 1693–1752.
10. J. Pushpamalar, A.K. Veeramachineni, C. Owh and X.J. Loh, Biodegradable polysaccharides for controlled drug delivery, *ChemPlusChem*, 2016, 81(6), 504 – 514.
11. H. Izawa, M. Nawaji, Y. Kaneko and J. Kadokawa, Preparation of glycogen-based polysaccharide materials by phosphorylase-catalyzed chain elongation of glycogen, *Macromol. Biosci.*, 2009, 9(11), 1098–1104.
12. S.A. Ferreira, P.J.G. Coutinho and F.M. Gama, Self-assembled nanogel made of mannan: synthesis and characterization, *Langmuir*, 2010, 26(13), 11413–11420.
13. H. Feng, X. Lu, W. Wang, N.G. Kang and J.W. Mays, Block copolymers: synthesis, self-assembly and applications, *Polymers*, 2017, 9(10), 494–525.
14. T. Aida, E.W. Meijer and S.I. Stupp, Functional supramolecular polymers, *Science*, 2012, 335(6070), 813–817.
15. S.I. Stupp, R.H. Zha, L.C. Palmer, H. Cui and R. Bitton, Self-assembly of biomolecular soft matter, *Faraday Discuss.*, 2013, 166, 9–30.
16. M.J. Webber and R. Langer, Drug delivery by supramolecular design, *Chem. Soc. Rev.*, 2017, 46, 6600–6620.
17. H. Cabral and K. Kataoka, Multifunctional nanoassemblies of block copolymers for future cancer therapy, *Sci. Technol. Adv. Mater.*, 2010, 11, 014109 (9 pp.).
18. R. Lin and H. Cui, Supramolecular nanostructures as drug carriers, *Current Opinion in Chemical Engineering*, 2015, 7, 75–83.
19. A. Pospisilova, S.K. Filippov, A. Bogomolova, S. Turner, O. Sedlacek, N. Matushkin, Z. Cernochova, P. Stepanek and M. Hruby, Glycogen-graft-poly(2-alkyl-2oxazolines) – the new versatile biopolymer-based thermoresponsive macromolecular toolbox, *RSC Adv.*, 2014, 4, 61580–61588.
20. R. Duncan, H.R. Gilbert, R.J. Carbajo and M.J. Vicent, Polymer masked–unmasked protein therapy. 1. Bioresponsive dextrin-trypsin and -melanocyte stimulating hormone conjugates designed for α -amylase activation, *Biomacromolecules*, 2008, 9(4), 1146–1154.

21. D. Hreczuk-Hirst, D. Chicco, L. German and R. Duncan, Dextrins as potential carriers for drug targeting: tailored rates of dextrin degradation by introduction of pendant groups, *Int. J. Pharm.*, 2001, 230, 57–66.
22. M. Vetric, M. Pradny, L. Kobera, M. Slouf, M. Rabyk, A. Pospisilova, P. Stepanek and M. Hruby, Biopolymer-based degradable nanofibers from renewable resources produced by freeze-drying, *RSC Adv.*, 2013, 3, 15282–15289.
23. K. Kim, W.C.W. Chen, Y. Heo and Y. Wang, Polycations and their biomedical applications, *Prog. Polym. Sci.*, 2016, 60, 18–50.
24. A.M. Alhoranta, J.K. Lehtinen, A.O. Urtti, S.J. Butcher, V.O. Aseyev and H.J. Tenhu, Cationic amphiphilic star and linear block copolymers: synthesis, self-assembly, and in vitro gene transfection, *Biomacromolecules*, 2011, 12(9), 3213–3222.
25. S. Has, H. Wan, D. Lin, S. Guo, H. Dong, J. Zhang, L. Deng, R. Liu, H. Tang and A. Dong, Contribution of hydrophobic/hydrophilic modification on cationic chains of poly(ϵ -caprolactone)-*graft*-poly(dimethylamino ethylmethacrylate) amphiphilic co-polymer in gene delivery, *Acta Biomater.*, 2014, 10(2), 670–679.
26. Y. Yang, F. Mo, Y. Chen, Y. Liu, S. Chen and J. Zuo, Preparation of 2-(dimethylamino) ethyl methacrylate copolymer micelles for shape memory materials, *J. Appl. Polym. Sci.*, 2015, 132(31), 42312–42319.
27. F.R. Mayo and F.M. Lewis, Copolymerization. I. A basis for comparing the behavior of monomers in copolymerization; the copolymerization of styrene and methyl methacrylate, *J. Am. Chem. Soc.*, 1944, 66(9), 1594–1601.
28. T. Kelen, F. J. Tudos, Analysis of the linear methods for determining copolymerization reactivity ratios. I. A new improved linear graphic method, *J. Macromol. Sci., A Chem.*, 1975, 9, 1–27.
29. M.T. Hunley, K.L. Beers, Nonlinear Method for Determining Reactivity Ratios of Ring-Opening Copolymerizations, *Macromolecules*, 2013, 46, 1393–1399.
30. I. Skeist, Copolymerization: the composition distribution curve, *J. Am. Chem. Soc.*, 1946, 68(9), 1781–1784.

6. Curriculum vitae

Name:	Mariia Rabyk
Date and place of birth:	31.12.1987, Lviv, Ukraine
Address:	Volavkova 1845/11, Praha 162 00, Czech Republic
Nationality:	Ukrainian
Telephone:	00420 777 504 094
E-mail:	rabyk@imc.cas.cz
Marital status:	married

Education

- from 10/2012** PhD studies at the Institute of Macromolecular Chemistry, Academy of Sciences of the Czech Republic (Department of Supramolecular Structures) under the supervision of RNDr. Petr Štěpánek, DrSc. and Mgr. Martin Hrubý, DSc. PhD thesis: “Functionalized hybrid polymer structures for biomedical applications”
- 07/2012-08/2012** Researcher at the Institute of Macromolecular Chemistry, Academy of Sciences of the Czech Republic (Department of Supramolecular Structures).
- 10/2011 – 07/2012** Scholarship holder, UNESCO/IUPAC postgraduate course in Advanced Polymer Science, Institute of Macromolecular Chemistry, Czech Academy of Science, Prague, “Stimuli responsive nanoparticles for biodiagnostic applications” (supervisor Ing. Jiří Pánek, PhD)
- 09/2009 – 11/2010** MSc studies at National University “Lviv Polytechnic”, Institute of Chemistry and Chemical Technologies. Diploma thesis: “Synthesis and properties of 4-substituted benzenthiosulfoacids esters”.
- 09/2005 – 06/2009** National University “Lviv Polytechnic”, Institute of Chemistry and Chemical Technologies, Chemical technology and engineering branch, BSc diploma in pharmacy.
- 09/1995 – 06/2005** Lviv Secondary School № 90, state medal award for excellent studies

Scientific experience

- 09/2007 – 09/2011** Research in laboratories of Department of Organic Chemistry and Department of Technology of Biologically Active Substances, Pharmacy and Biotechnology, National University “Lviv Polytechnic”
- 2009-2010** Member of the Young Scientist Council of Institute of Chemistry and Chemical Technologies

7. Publications and conference contributions

Publications included in the thesis

1. M. Jiratova, A. Pospisilova, M. Rabyk, M. Parizek, J. Kovar, A. Sekerkova, D. Jirak, M. Hruby, Biological characterization of a novel hybrid copolymer carrier system based on glycogen. *Drug Delivery and Translational Research*, 2017, 8(1), 73–82. IF = 3.09
2. M. Rabyk, A. Galisova, M. Jiratova, V. Patsula, L. Srbova, L. Loukotova, J. Parnica, D. Jirak, P. Stepanek, M. Hrubý, Mannan-based conjugates as multimodal imaging platform for sentinel lymph nodes. *Journal of Materials Chemistry B*, 2017, DOI: 10.1039/C7TB02888A. IF = 4.54
3. M. Rabyk, M. Hruby, M. Vetrik, J. Kucka, V. Proks, M. Parizek, R. Konefal, P. Krist, D. Chvatil, L. Bacakova, M. Slouf, P. Stepanek, Modified glycogen as construction material for functional biomimetic microfibers. *Carbohydrate polymers*, 2016, 152: 271–279. IF = 4.81
4. M. Rabyk, A. Destephen, A. Lapp, S. King, L. Billon, M. Hruby, O. Borisov, P. Stepanek, E. Deniau-Lejeune, Interplay of thermo- and pH-sensitivity of amphiphilic block gradient copolymers of 2-(dimethylamino)ethyl acrylate and styrene. *Macromolecules*, 2018, submitted. IF = 5.83

Other publications

1. L. Loukotova, J. Kucka, R. Konefal, M. Rabyk, M. Netopilik, P. Francova, L. Sefc, E. Mazl Chanova, P. Stepanek, M. Hruby, Hybrid thermoresponsive graft constructs of fungal polysaccharide β -glucan: physico-chemical and immunomodulatory properties, *European Polymer Journal*, 2018, submitted. IF = 3.53
2. L. Loukotova, J. Kucka, M. Rabyk, A. Hocherl, K. Venclikova, O. Janouskova, P. Paral, V. Kolarova, T. Heizer, L. Sefc, P. Stepanek, M. Hruby, Thermoresponsive β -glucan-based polymers for bimodal immunoradiotherapy - Are they able to promote the immune system? *Journal of Controlled Release*, 2017, 268, 78–91. IF = 7.78
3. V. Patsula, L. Kosinova, M. Lovric, L. Ferhatovic Hamzic, M. Rabyk, R. Konefal, A. Paruzel, M. Slouf, V. Herynek, S. Gajovic, D. Horak, Superparamagnetic Fe_3O_4 nanoparticles: synthesis by thermal decomposition of iron(III) glucuronate and application in magnetic resonance imaging, *ACS Applied Materials & Interfaces*, 2016, 8 (11), 7238–7247. IF = 7.5
4. V. Lobaz, M. Rabyk, J. Panek, E. Doris, F. Nallet, P. Stepanek, M. Hruby, Photoluminescent polysaccharide-coated germanium(IV) oxide nanoparticles, *Colloid and Polymer Science*, 2016, 294(7), 1225–1235. IF = 1.72
5. M. Vetrik, M. Pradny, L. Kobera, M. Slouf, M. Rabyk, A. Pospisilova, P. Stepanek, M. Hruby, Biopolymer-based degradable nanofibres from renewable resources produced by freeze-drying, *RSC Advances*, 2013, 3(35), 15282–15289. IF = 3.7
6. A. Bogomolova, M. Hruby, J. Panek, M. Rabyk, S. Turner, S. Bals, M. Steinhart, A. Zhigunov, O. Sedlacek, P. Stepanek, S. Filippov, Small-angle X-ray scattering and light scattering study of hybrid nanoparticles composed of thermoresponsive triblock copolymer F127 and thermoresponsive statistical polyoxazolines with hydrophobic moieties, *Journal of Applied Crystallography*, 2013, 46(6), 1690–1698. IF = 3.95
7. J. Panek, S. Filippov, M. Hruby, M. Rabyk, A. Bogomolova, J. Kucka, P. Stepanek, Thermoresponsive nanoparticles based on poly(2-alkyl-2-oxazolines) and pluronic F127, *Macromolecular Rapid Communications*, 2012, 33(19), 1683–1689. IF = 4.92

Conference contributions

Oral presentations

1. M. Rabyk, M. Jiratova, A. Galisova, D. Jirak, M. Hruby, Mannan conjugates for multimodal imaging, Nanotech France 2017, Paris, France. Book of abstract, Paris: SETCOR Conferences & Exhibitions, 2017. p. 103.
2. M. Rabyk, M. Parizek, M. Hruby, M. Vetric, J. Kucka, A. Pospisilova, P. Stepanek, Biodegradable glycogen-based nanostructures for biomedicine application, International Conference on Bio-Based Polymers and Composites /2./, Visegrad, Hungary, 2014. Programme Book, Budapest: Laboratory of Plastics and Rubber Technology, Budapest University of Technology and Economics, L-232.
3. M. Rabyk, J. Panek, M. Hruby, S. Filippov, A. Bogomolova, P. Stepanek, Stimuli responsive nanoparticles for biodiagnostic applications, Workshop "Career in Polymers IV". Prague, CR, 2012, Abstract Book, L2.

Poster presentations

1. M. Rabyk, M. Hruby, M. Vetric, J. Kucka, A. Pospisilova, P. Stepanek, Glycogen-based materials for tissue engineering. Workshop "Career in Polymers V". Prague, CR, 2013, Abstract Book, P8.
2. M. Rabyk, E. Deniau, L. Billon, O. Borisov, M. Hruby, P. Stepanek, Novel amphiphilic block-gradient copolymers of styrene and 2-dimethylaminoethyl acrylate. Self-assembly in the World of Polymers. PMM Conference /80./, Prague, CR, 2016, Book of Abstracts and Programme, p. 140, P-52.
3. M. Rabyk, E. Deniau, L. Billon, O. Borisov, M. Hruby, P. Stepanek, Synthesis and characterization of new amphiphilic block-gradient copolymers of styrene and 2-dimethylaminoethyl acrylate. Zjazd chemikov /69./. Horný Smokovec, Vysoké Tatry, SR, 2017, Book of abstracts, p.194, 6Po13.
4. M. Hruby, J. Kucka, J. Panek, H. Mackova, S. Filippov, A. Bogomolova, O. Sedlacek, M. Rabyk, R. Hoogenboom, B. Monnery, A. Ciolino, P. Stepanek, Thermoresponsive polymer micelles and nanoparticles: potential carriers of radiopharmaceuticals. Zjazd chemikov /65./. Tatranské Matliare, SR, 2013, Book of abstracts, p.104, 6PO1.
5. V. Lobaz, M. Rabyk, M. Hruby, J. Panek, P. Stepanek, Germanium and tungsten oxide nanoparticles for multimodal imaging. Workshop "Career in Polymers VII". Prague, CR, 2015, Book of abstracts, L1.
6. L. Loukotova, J. Kucka, M. Rabyk, A. Hoherl, K. Venclikova, O. Januskova, P. Paral, V. Kolarova, T. Heizer, L. Sefc, P. Stepanek, M. Hruby, Thermoresponsive β -glucan based polymers for immunoradiotherapy. Zjazd chemikov /69./. Horný Smokovec, Vysoké Tatry, SR, 2017, Book of abstracts, p.192, 6Po08.